ChemComm

Accepted Manuscript

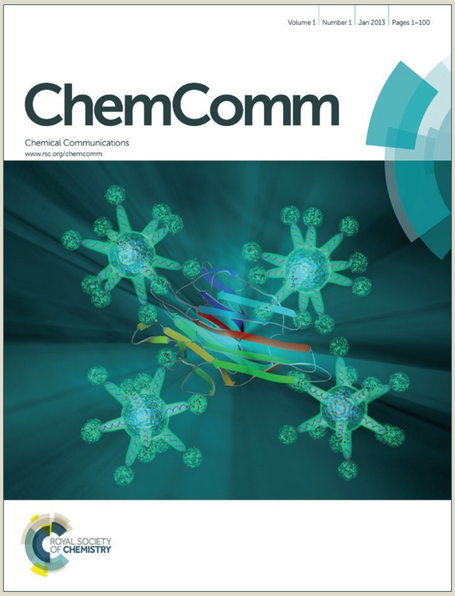

ROYAL SOCIETY OF CHEMISTRY

www.rsc.org/chemcomm

Journal Name RSCPublishing

COMMUNICATION

Cite this: DOI: 10.1039/x0xx00000x

Received 00th January 2012,
Accepted 00th January 2012

DOI: 10.1039/x0xx00000x

www.rsc.org/

Highly efficient and stable photocatalytic reduction of CO_2 to CH_4 over Ru loaded $NaTaO_3$

Mu Li,[ab] Peng Li,*[b] Kun Chang,[b] Tao Wang,[b] Lequan Liu,[c] Qing Kang,[b] Shuxin Ouyang[c] and Jinhua Ye*[abc]

An efficient and stable photocatalytic activity was obtained over $NaTaO_3$ by introducing electron donor (H_2) into the CO_2 reduction process with water. Ru/$NaTaO_3$ demonstrated the best activity (CH_4 51.8 μmol h^{-1} g^{-1}) and product selectivity in converting CO_2 to CH_4.

Ever since the profound Honda-Fujishima effect has been discovered by the early 1970s, semiconductor photocatalysis has received much attention as a potential solution to the worldwide energy shortage due to its promising ability in directly converting solar energy into chemical fuels.[1,2] In particular, photoreduction of CO_2 appears to be a highly fascinating process in lessening the requirement of fossil fuels and climate accommodation by atmospheric CO_2 balance. Generally, CO_2 reduction is a chain reaction with the product varying from CO ($2e^-$) to CH_4 ($8e^-$). Although the reduction potential of CH_4/CO_2 is about -0.24 V (vs. NHE at pH=7) which seems to be an attainable level to many semiconductors, CO_2 reduction has to go through a tough uphill process and its intermediates' redox potentials are much more negative ($E^{\theta}CO_2/CO$ = -0.61 V vs. NHE at pH=7).[3] Thus, to date, only a limited number of materials, such as $ZnGa_2O_4$,[4] Zn_2GeO_4,[5-7] $NaNbO_3$,[8-10] TiO_2,[11-13] etc., have exhibited photocatalytic activities in CO_2 reduction with various reducing outcomes. In the point view of products, CH_4 is more preferable when considering the high importance as a potential solar fuel.[14] But consequently, it enforces that the semiconductors must possess a negative enough conduction band (CB) to provide enough energy of the photogenerated electrons to overcome the activation barrier and fulfill the $8e^-$ reaction during the CO_2 reduction process.[11] $NaTaO_3$, which is one of the best pure water splitting photocatalysts reported by Kudo et al.,[15-17], possesses a significantly negative CB and analogous band gap to the above-mentioned semiconductors, likewise, should also bear a gigantic potential in CO_2 reduction, although there are few reports about it.

In previous researches, water was generally employed in reducing CO_2 as an active hydrogen source. However, although it is believed that CO_2 could react with H_2O to simultaneously produce CH_4 and O_2 through two respective half reactions with photogenerated electrons and holes in an ideal process,[5] O_2 could hardly be detected over most of the oxide semiconductors. It is usually accompanied by a decay of reactivity of CO_2 reduction reaction, since some peroxide intermediates could form and accumulate at the oxide semiconductor surface during the oxygen photoevolution reaction from water.[18] These peroxides would hinder the holes to oxidize the water and increase the recombination of the photogenerated electrons and holes, and consequently suppress the release of O_2. The unstable production rate has significantly limited the development and the practical application of CO_2 photoreduction. On the other hand, in the point view of reduction reaction, metal cocatalysts are commonly considered effective and broadly used in facilitating photocatalytic activities of semiconductors by (i) promoting the charge separation, (ii) improving the photostability, and (iii) lowering the activation energy of the catalytic reaction.[19,20] A recently attempt by Kang et al showed that the photocatalytic activity and stability can be significantly enhanced by replacing water with $N_2H_4\cdot H_2O$ as electron donor.[21] H_2 gas has also been confirmed that it can effectively facilitate the CO_2 reaction with water.[22-23] It opens a promising strategy to promote the photocatalytic efficiency and stability by using electron donor[11].

In this study, an electron donor (H_2 gas) was introduced to the reaction system to verify the peroxide intermediates mechanism during the water oxidation reaction and to enhance the activity as well as the stability of the CO_2 reduction. The effect of different metal cocatalysts for CO_2 photoreduction was studied with and without the electron donor, respectively. Among various metal cocatalysts loaded $NaTaO_3$ samples, Ru/$NaTaO_3$ (CH_4 51.8 μmol h^{-1} g^{-1}) and Pt/$NaTaO_3$ (CO 139.1 μmol h^{-1} g^{-1}) exhibited the best products selectivity in the presence of the electron donor. Moreover, Ru/$NaTaO_3$ showed a linear growth of CH_4 evolution over 24 hours and demonstrated an efficient and stable photocatalytic activity in converting CO_2 to CH_4. The key point of the performance over Ru/$NaTaO_3$ is owing to using H_2 as electron donor and distributing Ru as co-catalysts.

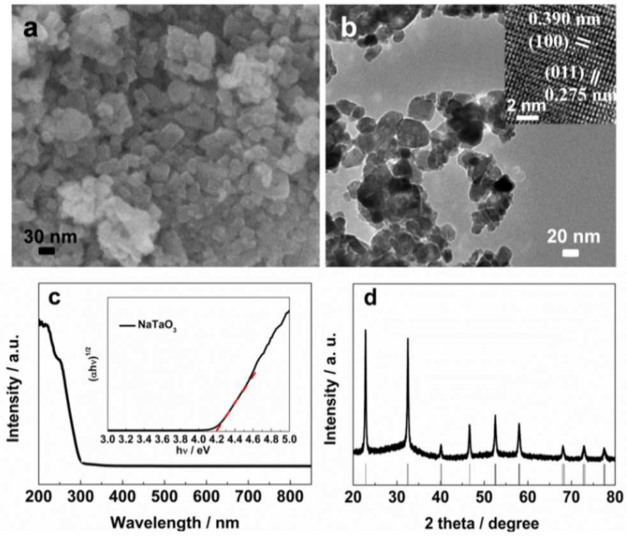

Fig. 1 (a) SEM image of $NaTaO_3$ sample; (b) TEM image of $NaTaO_3$ sample, the insert shows HRTEM image; (c) UV-vis absorption spectrum of $NaTaO_3$ sample and the inset is the corresponding $(\alpha h\nu)^{1/2}$– hν curve; (d) XRD pattern of $NaTaO_3$ sample.

The $NaTaO_3$ (NTO) samples were synthesized through a furfural alcohol derived polymerization–oxidation (FAPO) process.[8,9] The detailed characteristics were examined by X-ray diffraction (XRD), ultraviolet-visible (UV-vis) spectroscopy, scanning electron microscope (SEM) and transmission electron microscopy (TEM). The XRD pattern (Fig. 1d) and its corresponding HRTEM (insert in Fig. 1b) show that the $NaTaO_3$ prepared through the FAPO route crystallized in a monoclinic system with the space group of *P2/m*, which could be well indexed to the JCPDS database card (JCPDS-01-074-2477). According to the SEM and TEM images (Fig. 1a and 1b), the sample mainly contains particles about 20 ~ 30 nm. UV-visible absorption spectrum of the $NaTaO_3$ nanoparticles is shown in Fig.1c, with an intense absorption with steep edge in the UV region. The band gap (E_g) of $NaTaO_3$ was determined to be 4.2 eV according to the following equation $(\alpha h\nu)^{1/2} = A(h\nu - E_g)$ and shown in the inset of Fig.1c, in which α, ν, A, and E_g are the absorption coefficient, light frequency, proportionality constant and band gap, respectively.

The photocatalytic properties of the as-prepared $NaTaO_3$ were estimated by photoreduction of gaseous phase CO_2 under the irradiation of a 300 W UV-enhanced Xe lamp. Fig. 2a and Fig. 2b exhibit the results of CO_2 reduction over the series of $NaTaO_3$ only using water as the reducing agent. All the samples showed certain abilities, where CH_4 and CO presented to be the two main carbon products as well as some trace amount of other hydrocarbon compounds (Fig. S11) with CO appears more dominant. The total productivities were listed in Table S2. Metal cocatalysts mainly benefited H_2 evolution in this reaction condition (CO_2+H_2O), because H_2 evolution is a highly preferred competing reaction. The CO_2 reduction reactions exhibited not linear growth of the products evolution. The bent curves indicate an unstable reactivity of CO_2 reduction reaction for all the samples. Moreover, O_2 could also not be detected as the product of water oxidation. Thus, an obstructive O_2 release process should be the main reason for the above phenomena. It has been reported that some peroxide intermediates would be formed at the oxide semiconductor surface during the oxygen photoevolution reaction from water.[18] As shown in Fig. 2c, the intermediates are proved to be generated by the in situ FTIR spectra. By referring the method reported in the literature,[18] $NaTaO_3$ film was exposed to a 30% H_2O_2 aqueous solution to position the peak of peroxide intermediates (dot line), the peaks at 834 cm^{-1} and 883 cm^{-1} belong to the peroxide intermediates and H_2O_2, respectively. During the CO_2 reduction process, the peroxide intermediates formed and accumulated with the time when only using water as the reducing agent (dash line). As the schematic model shown in Fig. 2d, the peroxide intermediates hindered the photogenerated holes to oxidize water. Consequently, the recombination of electrons and holes increased, and so that reflects on a decreased photocatalytic activity.

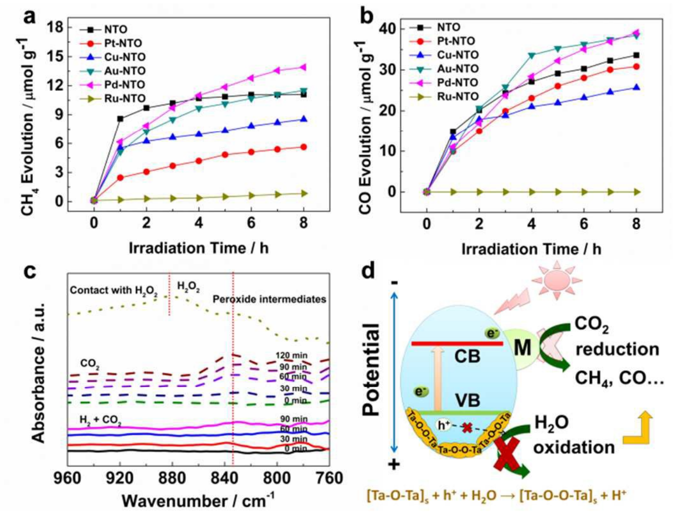

Fig. 2 Gaseous product generation over 0.5 wt% co-catalysts loaded $NaTaO_3$ in H_2O and CO_2 atmosphere: (a) CH_4, (b) CO; (c) In situ FTIR spectra of $NaTaO_3$ during the CO_2 reduction process; (d) Schematic model of the formation and accumulation of peroxides at the surface of $NaTaO_3$.

In order to eliminate the hamper of peroxide intermediates and realize a stable reduction of CO_2, an electron donor (H_2 gas) was introduced to the reaction system to release the peroxides. Fig. 3a and 3b show the results of CO_2 reduction over the series of $NaTaO_3$ in the presence of H_2O, CO_2 and H_2. All the samples exhibit promotions of the catalytic activity compared with the counterparts only using H_2O and CO_2 as shown in Table S2. Almost linear curves indicate that enhanced stabilities and activities of the CO_2 reduction are obtained over the catalysts, especially for Ru/ $NaTaO_3$ (Fig. S4a). As the solid lines in Fig. 2c shown, there is almost no accumulation of the peroxides in the presence of electron donor H_2. It can be concluded that the peroxide intermediates are effectively reduced by H_2 and so that a stable reduction of CO_2 are observed. An isotope experiment within a D_2O, CO_2 and H_2 atmosphere was carried out to distinguish the hydrogen source between water (D_2O) and H_2 of the produced methane. Initially, CD_4 is the dominant methane products (Fig. S2a), which illustrates clearly that the hydrogen in methane comes from water (D_2O). With the reaction proceeded after several hours, some CD_3H and CD_2H_2 can be observed among the methane products (Fig. S2b). It is deduced that the protium atoms should mainly derive from the normal water (H_2O) reduced from peroxides at $NaTaO_3$ surface by

H_2 Thus, it is confirmed that the direct hydrogen source of the CO_2 reduction is still water, but not the H_2 gas introduced as the electron donor. H_2 promotes the CO_2 reduction reaction by a successful conversion of peroxide intermediates (O_2^*) into water rather than directly reduces CO_2 to CH_4 as the schematic model shows in Fig. 3d. This is because that the requisite active hydrogen to react with CO_2 in a photocatalytic process should be atomic hydrogen rather than molecular hydrogen. The hydrogenation reaction between molecular hydrogen and CO_2 must climb over an energy barrier to push forward,[25,26] where the requirement could not be met in this work. The atomic hydrogen is activated from other hydrogen sources (water in this work), although there are hydrogen molecules in the system.[21]

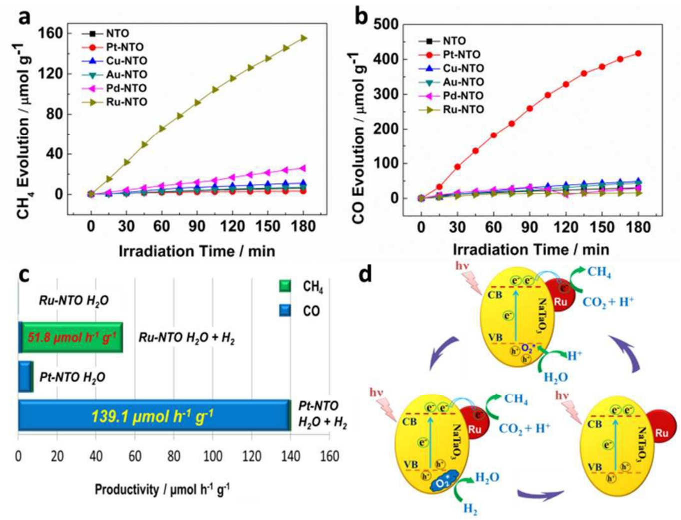

Fig. 3 Gaseous product generation over 0.5 wt% co-catalysts loaded $NaTaO_3$ in CO_2, H_2O and H_2 atmosphere: (a) CH_4, (b) CO; (c) Productivity with and without H_2 over Ru-$NaTaO_3$ and Pt-$NaTaO_3$; (d) Schematic model of a proposed reaction process of Ru-$NaTaO_3$ in CO_2, H_2O and H_2 atmosphere.

In the point view of cocatalyst, except for Ru and Pt, other cocatalysts did not exhibit a pronounced activity enhancement and selectivities of CO_2 reduction due to their natural properties as shown in Table S2. Ru/$NaTaO_3$ (CH_4 51.8 μmol h^{-1} g^{-1}) and Pt/$NaTaO_3$ (CO 139.1 μmol h^{-1} g^{-1}) exhibited the best activities and products selectivity over the series (Fig. 3a and Fig. 3b). The CH_4 or CO versus total carbon products (CH_4 + CO) ratio is about 0.96 for Ru/$NaTaO_3$ and 0.99 for Pt/$NaTaO_3$ (Fig. 3c). These results accord well with the results in the literatures.[26 - 28] It is mainly attributed to the excellent abilities of Ru and Pt in hydrogen activation, stabilization and utilization, since these two metals are commonly used materials for hydrogen storage[29,30] and fuel cells.[31,32] Since converting CO_2 to CH_4 is a multiple-step and multiple-electron reaction (Fig. S3), there must be an inexhaustible supply of active hydrogen (H^*) to CO_2. CO molecules possess dominant adsorption ability than H_2O at Pt surface.[33] After CO_2 molecules have been reduced to CO, the supply of active hydrogen decrease gradually until the Pt surface was fully occupied by CO and finally poisoned by them.[33,34] Thus, the CO_2 reduction over Pt predominantly carries out a $2e^-$ reaction and CO become the main product. Conversely, water molecules are more adsorptive at Ru surface,[33] and Ru has a relative high overpotential in H_2 evolution[35] to depress the H^* recombining to H_2. Thus, active hydrogens could be constantly provided to CO_2 to carry out $8e^-$ reaction. In addition, the state of Ru is also very important to the activity. Different from other noble metals, Ru is very easy to be oxidized during the drying process. Moreover, this oxidation might be even enhanced when only using water as the reductant due to the formation of $Ru(OH)_{ads}$.[32,33] Thus, the real state of the cocatalysts should be a mixture of Ru and RuO_2 or RuO_x (Fig. 4a). The partially oxidized RuO_x not only hinder the electron transfer from $NaTaO_3$ to Ru, but also weaken the hydrogen activation on metal Ru. So that it lead to a very poor activity (Fig. 1). However, after introducing the electron donor H_2, RuO_x could be reduced and transformed to metal Ru again (Fig. 4). As the XPS spectra shown in Fig.4b, Ru oxides in the as-prepared Ru-$NaTaO_3$ were reduced to metal Ru. The corresponding TEM image (Fig.4c and 4d) also indicates the successful transformation to metal Ru. Thus, a stable CO_2 reduction can be ensured over Ru/$NaTaO_3$.

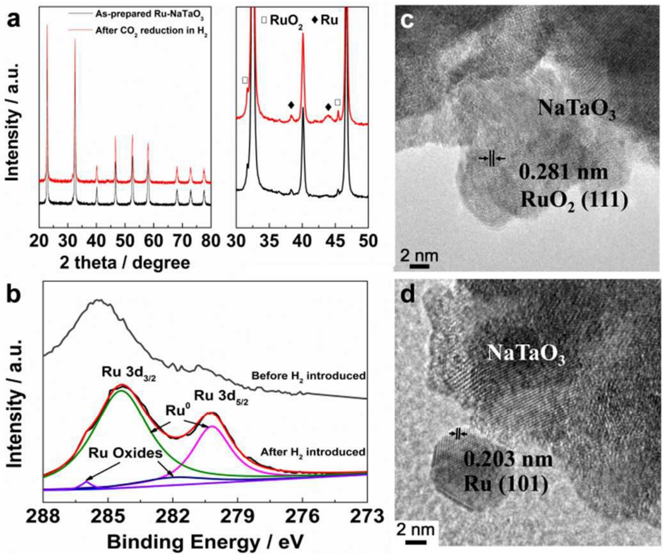

Fig. 4 (a) XRD patterns of Ru/$NaTaO_3$ samples. Black line: as-prepared Ru/$NaTaO_3$, Red line: Ru/$NaTaO_3$ after a CO_2 reduction under H_2 atmosphere. □ RuO_2, ◆ Ru. 10 wt% Ru/$NaTaO_3$ was adopted for better observation of the responds of RuO_2 and Ru. (b) XPS spectra of Ru/$NaTaO_3$ before and after CO_2 reduction in H_2 atmosphere. TEM image of (c) as-prepared Ru/$NaTaO_3$; (d) Ru/$NaTaO_3$ after CO_2 reduction in H_2 atmosphere.

Long-playing experiments were carried out to examine the stabilities of these two samples, respectively (Fig. S4). Ru/$NaTaO_3$ keeps a linear growth of CH_4 evolution even overnight, whereas Pt/$NaTaO_3$ exhibits a decay of CO evolution after several hours due to the poisoning of Pt by the produced CO.[33,34] Further experiments were also carried out to confirm the light dependent photocatalytic activity (Fig. S5). Both Ru/$NaTaO_3$ and Pt/$NaTaO_3$ expressed obviously feedbacks, i.e., the reactions exhibit very poor activities under visible light irradiation and there were hardly increases of the products until the L42 filter was removed. Thus, it could be definitely concluded that CO_2 was photocatalytically reduced over Ru/$NaTaO_3$ and Pt/$NaTaO_3$, as $NaTaO_3$ is a wide band-gap semiconductor (4.2 eV). An isotope experiment was carried out over Ru/$NaTaO_3$ for further investigation using $^{13}CO_2$. The GC-MS spectrum exactly confirmed that the organic product $^{13}CH_4$ was reduced from $^{13}CO_2$ (Fig. S6).

In addition, Ru loaded $SrTiO_3$ and TiO_2 also exhibit stable photocatalytic activities of converting CO_2 to CH_4 in the presence of electron donor H_2 (Fig. S7a). The activity differences among $NaTaO_3$, $SrTiO_3$ and TiO_2 are mainly attributed to their different CB levels (Fig. S7 and Fig. S8). Moreover, these results demonstrate that electron donor could also be extended to other semiconductors to realize a stable photoreduction of CO_2. Some other electron donor will be studied to substitute H_2 in the following work.

In conclusion, this study demonstrated that the phototcatalytic activities of $NaTaO_3$ are greatly affected by reducing agents and cocatalysts. By introducing electron donor H_2 into the system, a stable reactivity has been obtained over the series of $NaTaO_3$ due to an effective release of the peroxides intermediates of water oxidation. Ru/$NaTaO_3$ (CH_4 51.8 μmol h^{-1} g^{-1}) and Pt/$NaTaO_3$ (CO 139.1 μmol h^{-1} g^{-1}) exhibited the best products selectivity in the presence of the electron donor. Besides, Ru demonstrated an efficient and stable photocatalytic activity in converting CO_2 to CH_4 beyond 24 hours. These results and discussion reveal that as co-catalysts, Ru possesses an efficient ability to promote the photogenerated charge separation as well as the hydrogen activation, stabilization and utilization in the presence of electron donor in photoreducing CO_2 to CH_4.

This work was partly supported by World Premier International Research Center (WPI) Initiative on Materials Nanoarchitectonics (MANA), MEXT, Japan, and National Basic Research Program of China (973 Program, 2014CB239301). M. Li gratelfully acknowledges financial support from China Scholarship Council (CSC). The author thanks Dr. H. Iwai and Dr. A. Tanaka from Materials Analysis Station, National Institute for Materials Science (NIMS) for XPS measurements.

Notes and references

a Graduate School of Chemical Sciences and Engineering, Hokkaido University, Sapporo, Japan. E-mail: Jinhua.YE@nims.go.jp
b Environmental Remediation Materials Unit and International Center for Materials Nanoarchitectonics (WPI-MANA), National Institute for Materials Science, 1-1 Namiki, Tsukuba, Ibaraki 305-0044 (Japan) E-mail: LI.Peng@nims.go.jp
c TU-NIMS Joint Research Center, School of Materials Science and Engineering, Tianjin University, 92 Weijin Road, Nankai District, Tianjin, P. R. China.

† Electronic Supplementary Information (ESI) available: [Experimental, supplementary activity characterization, isotope experiments, etc]. See DOI: 10.1039/c000000x/

(1) Fujishima, A.; Honda, K. *Nature* **1972**, *238*, 37–38.
(2) Tong, H.; Ouyang, S.; Bi, Y.; Umezawa, N.; Oshikiri, M.; Ye, J. *Adv. Mater.* **2012**, *24*, 229–251.
(3) Kumar, B.; Llorente, M.; Froehlich, J.; Dang, T.; Sathrum, A.; Kubiak, C. P. *Annu. Rev. Phys. Chem.* **2012**, *63*, 541–569.
(4) Yan, S. C.; Ouyang, S. X.; Gao, J.; Yang, M.; Feng, J. Y.; Fan, X. X.; Wan, L. J.; Li, Z. S.; Ye, J. H.; Zhou, Y.; Zou, Z. G. *Angew. Chem. Int. Ed.* **2010**, *49*, 6400–6404.
(5) Liu, Q.; Zhou, Y.; Kou, J.; Chen, X.; Tian, Z.; Gao, J.; Yan, S.; Zou, Z. *J. Am. Chem. Soc.* **2010**, *132*, 14385–14387.
(6) Zhang, N.; Ouyang, S.; Li, P.; Zhang, Y.; Xi, G.; Kako, T.; Ye, J. *Chem. Commun.* **2011**, *47*, 2041–2043.
(7) Yan, S.; Wan, L.; Li, Z.; Zou, Z. *Chem. Commun.* **2011**, *47*, 5632–5634.
(8) Li, P.; Ouyang, S.; Xi, G.; Kako, T.; Ye, J. *J. Phys. Chem. C* **2012**, *116*, 7621–7628.
(9) Li, P.; Ouyang, S.; Zhang, Y.; Kako, T.; Ye, J. *J. Mater. Chem.* **2013**, *1*, 1185–1191.
(10) Li, P.; Xu, H.; Liu, L.; Kako, T.; Umezawa, N.; Abe, H.; Ye, J. *J. Mater. Chem.* **2014**, *2*, 5606–5609.
(11) Habisreutinger, S. N.; Schmidt-Mende, L.; Stolarczyk, J. K. *Angew. Chem. Int. Ed.***2013**, *52*, 7372–7408.
(12) Xu, H.; Ouyang, S.; Liu, L.; Wang, D.; Kako, T.; Ye, J. *Nanotechnology* **2014**, *25*.
(13) Wang, T.; Meng, X.; Li, P.; Ouyang, S.; Chang, K.; Liu, G.; Mei, Z.; Ye, J. *Nano Energy* **2014**, *9*, 50–60.
(14) Sastre, F.; Puga, A. V.; Liu, L.; Corma, A.; García, H. *J. Am. Chem. Soc.* **2014,** *136,* 6798–6801.
(15) Kato, H.; Kudo, A. *J. Phys. Chem. B* **2001**, *105*, 4285–4292.
(16) Kato, H.; Asakura, K.; Kudo, A. *J. Am. Chem. Soc.* **2003**, *125*, 3082–3089.
(17) Yamakata, A.; Ishibashi, T.; Kato, H.; Kudo, A.; Onishi, H. *J. Phys. Chem. B* **2003**, *107*, 14383–14387.
(18) Nakamura, R.; Nakato, Y. *J. Am. Chem. Soc.* **2004**, *126*, 1290–1298.
(19) Yang, J.; Wang, D.; Han, H.; Li, C. *Accounts Chem. Res.* **2013**, *46*, 1900–1909.
(20) Zhou, H.; Guo, J.; Li, P.; Fan, T.; Zhang Di.; Ye, J. *Sci. Rep.* **2013**, *3*.
(21) Kang, Q.; Wang, T.; Li, P.; Liu, L.; Chang, K.; Li, M.; Ye, J. *Angew. Chem. Int. Ed.* **2015**, *54*, 841–845.
(22) Tsuneoka, H.; Teramura, K.; Shishido, T.; Tanaka, T. J. Phys. Chem. C 2010, 114, 8892–8898.
(23) Teramura, K.; Tanaka, T.; Ishikawa, H.; Kohno, Y.; Funabiki, T. J. Phys. Chem. B 2003, 108, 346–354.
(24) Kohno, Y.; Tanaka, T.; Funabiki, T.; Yoshida, S. Chem. Commun. 1997, 841–842.
(25) Wang, W.; Wang, S.; Ma, X.; Gong, J. *Chem. Soc. Rev.* **2011**, *40*, 3703–3727.
(26) Meng, X.; Wang, T.; Liu, L.; Ouyang, S.; Li, P.; Hu, H.; Kako, T.; Iwai, H.; Tanaka, A.; Ye, J. *Angew. Chem. Int. Ed.* **2014**, *53*, 11478–11482.
(27) Azuma, M.; Hashimoto, K.; Hiramoto, M.; Watanabe, M.; Sakata, T. *J. Electrochem. Soc.* **1990**, *137*, 1772–1778.
(28) Lee, J.; Kwon, Y.; Machunda, R. L.; Lee, H. J. *Chem. – Asian J.* **2009**, *4*, 1516–1523.
(29) Wang, L.; Yang, R. T. *J. Phys. Chem. C* **2008**, *112*, 12486–12494.
(30) Saha, D.; Deng, S. *Langmuir* **2009**, *25*, 12550–12560.
(31) Oetjen, HF.; Schmidt, V. M.; Stimming, U.; Trila, F. *J. Electrochem. Soc.* **1996**, *143*, 3838–3842.
(32) Liu, H.; Song, C.; Zhang, L.; Zhang, J.; Wang, H.; Wilkinson, D. P. *J. Power Sources* **2006**, *155*, 95–110.
(33) Yajima, T.; Uchida, H.; Watanabe, M. *J. Phys. Chem. B* **2004**, *108*, 2654–2659.
(34) Wakisaka, M.; Ohkanda, T.; Yoneyama, T.; Uchida, H.; Watanabe, M. *Chem. Commun.* **2005**, 2710–2712.
(35) Bard, A. J.; Faulkner, L. R. *Electrochemical Methods: Fundamentals and Applications*; Wiley, 2001.